Deliverable

WP1 – Materials preparation and design of the PMP/PZL devices

D1.1 Guidelines for the materials evaluation of PMP films, of the PMP encapsulation process and of the PZL device

Project Information

Grant Agreement n°	863227
Dates	01-12-2019 / 30-11-2022

This project has received funding from the European Union's Horizon 2020 research and innovation programme under grant agreement No 863227.

Document status

Document Information

Deliverable name	PULSE-COM_D1.1_20032021_RF
Responsible beneficiary	Riccardo Castagna / CNR
Contributing beneficiaries	ENEA, UGA, INFLPR RA, CBRTP S.A.
Contractual delivery date	M4 - 31/03/2020
Actual delivery date	M4 - 20/03/2021
Dissemination level	Public

Document approval

Name	Position in project	Organisation	Date	Visa
Lucia Petti	Coordinator	CNR	20/03/2021	OK
Riccardo Castagna	WP Leader	CNR	/03/2021	
Jean Herisson	Project Management Officer	AYMING	22/03/2021	OK
Fabienne Brutin	Project Management Officer	AYMING	22/03/2021	OK

Document history

Version	Date	Modifications	Authors
V0	27/02/2020	Draft version	R. Castagna/B. Sava/G. Nenna/G. Ardila Rodriguez
V1	28/02/2020	Few modifications	L.Petti / CNR
V2	02/03/2020	Adaptation to the graphical chart	J.Herisson / AYMING
V3	05/03/2020	Comments on section 5	L. Petti/CNR, G. Nenna/ENEA
V4	19/03/2020	Integration	R. Castagna/B. Sava/ G. Ardila Rodriguez
V5	21/03/2020	Revision	L. Petti/CNR, G. Nenna/ENEA
V6	25/03/2020	Further revisions	L. Petti/ R. Castagna CNR
VF	27/03/2020	Final revisions	J.Herisson / G. Ardila Rodriguez / L. Petti / R. Castagna
RV	17/03/2021	Revised after Monitoring evaluation	G.Nenna / L. Petti / R. Castagna
RF	20/03/2021	Final Revision after Monitoring evaluation	J.Herisson/G.Nenna / L. Petti

Table of content

List of Figures

Executive summary

1 Description of the deliverable content and purpose

The objective of this deliverable is to report on the guidelines for the materials evaluation of PMP films, of the PMP encapsulation process and of the PZL device after an extended and detailed research on the PMP polymers, PZL materials and encapsulation process present in the literature and commercially available. This is necessary to ensure the most appropriate material characteristics suitable for the realization of the project. The possibility to use hazardous materials was examined to guarantee the final disposal of end-of-life devices or process waste to protect the environment.

Deliverable report

1 Brief Introduction

Our project intends to produce piezo-electro-photonic devices by unifying two concepts: (i) the conversion of photon energy into mechanical work by means of a photo-mobile polymer film (PMP), which is usually a plastic film of which the deformations can be induced and controlled by wavelength, polarization, intensity, density, angle of incidence of an impinging coherent and/or uncoherent light and (ii) the conversion of mechanical energy into electrical energy by means of a piezo-electric material. Our goal, in particular, is to obtain highly efficient photo-piezo-electric-actuators, namely piezo-actuators stimulated by different light sources and/or by sun light, to open a new paradigm in the harvesting energy field and sensing. In extreme synthesis, we intend to transform photonic-energy into mechanical work (by a polymeric film) and, subsequently, by using the same device, the mechanical work into electricity (by a piezoelectric film).

2 State of the Art: the nearest approaches to PULSE-COM concept

In the state of the art our approach simply doesn't exist. As far as we know, there is only one approach in literature that could recall - at a glance - our project/proposal. It is based on a metal-silicon supported device. [1] It converts photon-energy into heat and, as consequence, generates micro-deformation on the metal structure producing electricity throughout a piezo-system. However, the described device is very distant from our project/proposal since: a) conceptually, we intend to transform directly light-/photon-energy into mechanical work, by using PMPs and without dispersive (heating) intermediate steps; b) we propose efficient large-area (cm^2) and meso-scale systems, having large-bending angles and high oscillation frequencies; c) finally, in the cited document, the reversibility of the system, necessary for the working activity of the device is not reported (neither understandable from the text). On the other hand, piezoelectric materials are widely used for mechanical to electric energy conversion. The nearest approach to our project/proposal is based on mechanical stretching of piezo-films (PZL) that is realized by many different techniques and in particular by using flexible substrates. [2] They generate electric power from vibrations or by mechanical inputs associated with movements of the human body or machines and environmental natural sources, such as waves or wind. Here, recent capabilities in rendering piezoelectric devices in thin, mechanically ‘soft’ formats are critically important. Moreover, the realization of piezoelectric devices usually takes a number of steps using temperature processes and organic solvents. For this reason an opportune encapsulation process has to be adopted to protect the photopolymer film in order to maintain intact its photo-mobile properties and to work at relatively high temperatures and in different solvents, and to guarantee for example the Zinc Oxide (ZnO) nanowires growth that is used in PULSE-COM as piezoelectric material. It follows that the photomobile polymer must be able to withstand this type of conditions.

3 Regarding the Piezo Layers (PZLs) suitable for this project (State of the Art)

The integration of a piezoelectric material into a flexible substrate, in particular a polydimethylsiloxane (PDMS)-like polymer, requires special attention firstly to the temperature of fabrication of the active material not exceeding 200°C and secondly, to

ensure the right mechanical properties to the staked device, for instance to avoid unwanted mechanical load on the application or to reach high degrees of bendability without reducing excessively the electrical energy generated. [2] The classical techniques to fabricate high performing perovskites like PZT or PMN-PT cannot be used in this case as they require high temperature to be developed (~ 1000°C). In the state of the art, several approaches have been proposed to integrate different piezoelectric materials, mostly nano-composites into flexible substrates. For instance, PZT nanoribbons fabricated on a rigid substrate and then reported on PDMS [3] or Lead Magnesium Niobate - Lead Titanate (PMN-PT) nanostructures dispersed in PDMS before been spin-coated into a flexible substrate. [4] These two examples show that the piezoelectric material can be fabricated without exposing the substrate to high temperatures; on the other hand, these two materials contain Lead which is toxic and is actually being regulated by the European Union in electrical and electronic equipment (RoHS and RoHS2 for Restriction of Use of Hazardous Substances). [5] Other materials not containing Lead have been also integrated into flexible substrates: i) polyvinylidene fluoride (PVDF) and its copolymer, poly(vinylidene fluoride–trifluoroethylene) (PVDF–TrFE) processed as aligned fibers by electrospinning. [6] Its counterpart thin film deposited by spin-coating [7] is particularly interesting because the ease of fabrication/deposition although its coupling coefficients is not too high (d33 ~ 15 pm/V, here d33 represent the relation between the displacement and voltage measured along the same direction. It is important to note that under bending, several piezoelectric modes are used, in particular d33 and d31, we discuss here only d33 for comparison between materials); ii) Barium Titaniate ($BaTiO_3$) nanowires (NWs) and nanotubes synthesized via Chemical Bath Deposition (CBD) and dispersed into PDMS, before being spin-coated into the flexible substrate [8]. Although their coupling coefficient is higher (d33 ~ 460 pm/V), their fabrication is relatively more complex and longer (several days) compared to other NWs like Zinc Oxide (ZnO), poling is also necessary in the final device (an application of a high voltage ~1 kV for 12 h at 140°C). iii) Aluminium Nitride (AlN) thin film deposited by radio frequency magnetron sputtering method at temperatures close to room temperature [9, 10], providing lower coupling coefficients (d33 ~ 0.7 pm/V) because of its low crystallinity quality. iv) ZnO NWs vertically grown by CBD and either used laterally dispersed into a polymer matrix before being deposited by spin-coating into the flexible substrate [11] or vertically for their immersion into a matrix material [12]. This last is probably the most explored technique to develop piezo-composites, it is very attractive because of the ease of fabrication of the NWs using CBD not requiring expensive and long methods. It is also reported that the piezoelectric coupling coefficient of ZnO nanostructures (d33 ~ 26 pm/V) [13] are about 2 times higher than their thin film counterparts which explains also their interest.

The vertical integration of ZnO NWs into composites for electromechanical energy transduction applications such as sensing and energy harvesting have been studied by many research groups in the last decade. The basic structure of the piezoelectric composite can be seen in Figure 1. It is composed of a rigid or a flexible substrate, a bottom electrode, a ZnO seed layer, the NWs which are immerged in a dielectric matrix and a top electrode. It is commonly known as the VING (Vertically Integrated Nano Generator) configuration. In most of the reported works, the ZnO NWs were grown using CBD (Chemical Bath Deposition also known as hydrothermal growth) [14] and immerged in a polymer matrix being polymethyl-methacrylate (PMMA) or PDMS deposited by spin-coating, and were characterized under compressive forces [14]. The VING configuration was first used in mechanical energy transduction in 2010 by Prof. Z. L. Wang group in GeorgiaTech. [15] In this Initial device the tips of the NWs were contacted directly to the top electrode made of Pt creating a Schottky contact. One single device evaluated under compression generated about 80 mV. Then, several devices could be placed one on top of each other and connected

in series increasing the potential up to ~ 0.2 V. Contacting all the tips of the NWs is not easy and could reduce the device performance. One solution to this issue was proposed in [16], where the authors added a thin dielectric layer between the NWs and the top electrode (as depicted in Figure 1). This technique has been used in most articles since then as it facilitates the integration and adds robustness to the device. In that article, the authors integrated the composite (ZnO inside a PMMA matrix) on both sides of a 220 µm thick flexible film of polyester (PS) and added Cr/Au top electrodes. The device was finally encapsulated using PDMS. The device produced up to 10 V under 0.12% strain and strain rate of 3.56% S^{-1}. Since then, some other works have been reported on devices integrating the piezo composite on flexible substrates and being evaluated under bending forces. One of those reported works was developed in collaboration with UGA partner (IMEP-LaHC laboratory) [11]. In that work, the piezo composite (ZnO NWs immerged in PMMA) was integrated on a thin aluminium substrate (~ 18 µm) and used as mechanical sensor to track the eye ball movement (Figure 2). This device generated ~ 120 mV under mechanical bending (not quantified here). In [17] Dahiya *et al.* integrated the piezo composite on a PDMS substrate and used Parylene C as matrix material. Parylene C was deposited using room temperature vapor-phase deposition. The device was mainly tested under compression. Bending tests were also reported by attaching the device to a finger. When the finger bent the device, it provided voltages between 2 V and 4 V. In [18], the authors integrated on a Polyimide (PI) flexible substrate, a piezo composite made of vertical ZnO NWs immerged into PVDF which is a ferroelectric polymer. The authors used Cr/Au as bottom and top electrode. A poling process at high voltage (1.2 MV/cm) was necessary to polarize the PDVF. The device produced up to 0.4 V at 3% strain. Further devices were focalized on the improvement of performances. In [19], Hu *et al.* used the architecture proposed in [15] but changed the substrate from PS to Kapton which sustain higher temperature. The authors tested several procedures: i) exposure of the NWs to O_2 plasma, ii) annealing at 350°C for 30 min, ii) surface passivation using polymers, in this case by coating first with positive charged poly-(diallydimethylammonium chloride) (PDADMAC) and then by negatively charged poly-(sodium 4-styrenesulfonate) (PSS) through a layer-by-layer self-assembly method. They found that this last method was the most effective and increased the output potential to 20 V under bending. In other reports, flexible devices were fabricated on poly-ethylene/Indium Tin Oxide (PET/ITO) substrate and replaced the PMMA in the matrix by a p-type polymer poly-(3,4-ethylenedioxythiophene): poly-(styrenesulfonate) (PEDOT:PSS) contacting only the NWs tips, creating a p-n junction. Although these devices produced a lower voltage compared to previous ones under bending (~ 10 mV), the internal resistance is lower than previous devices, thus transferring eventually more power to an external load ($P = V^2/R$). Later it was shown that using a more conductive p-type polymer poly-(3,4-ethylenedioxythiophene-Tosylate) (PEDOT:Tos), a higher voltage (~ 1 V) was generated compared to PEDOT:PSS [20, 21].

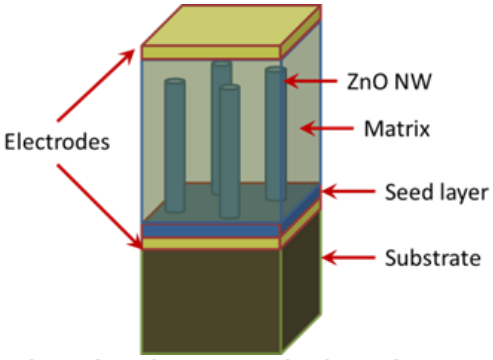

Figure 1: Basic structure of the piezoelectric composite based on ZnO NWs immerged in a dielectric matrix.

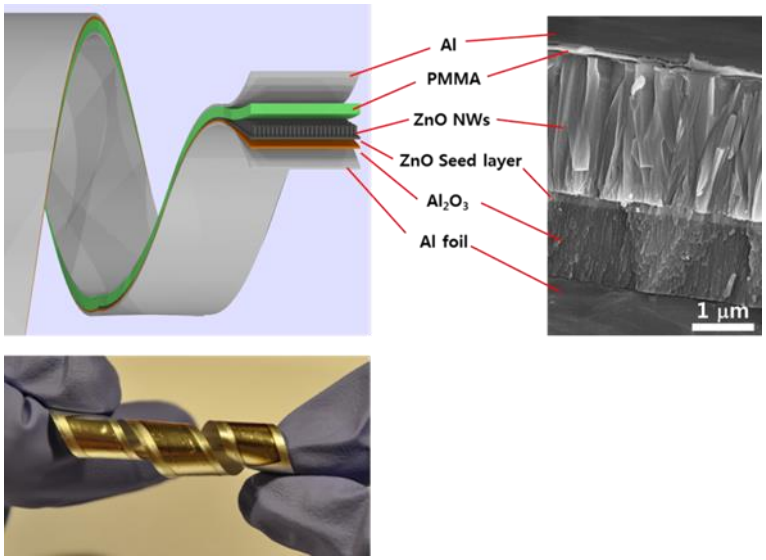

Figure 2: Example of integration of the piezo composite on flexible substrates [15].

From a theoretical point of view, very few research groups have studied the piezoelectric composite based on vertical ZnO NWs. In [22], Graton *et al.* developed an equivalent circuit model of VING under compressive forces taking into account the effect of the polymer matrix to simulate the electromechanical behavior of the device. The simulation results were in good agreement with values from literature.

In [23], Hinchet *et al.* developed analytical and Finite Element Method (FEM) models coupling mechanical, piezoelectric and electrostatic physics to evaluate the composite under a compressive force. They found several ways to improve the device performance: i) using a soft material like PMMA as matrix, ii) reducing the thickness of the layer between the tip of the NWs and the top electrode and iii) improving the piezoelectric coefficients of the NWs. In a later article [24], Hinchet *et al.* used similar models to evaluate, in particular the effect of the NWs density in the device performance. To simplify the models, the authors studied an individual cell (i.e. a single NW immerged in the polymer as unit cell of the whole device) (Figure 3a). The density was defined in the models as the ratio between the diameter of the NWs and the width of the individual cell (Figure 3b). They found that i) a medium density of NWs increased the overall performance and ii) the composite performance was better (x 3.3) compared to a ZnO thin film (Figure 3c).

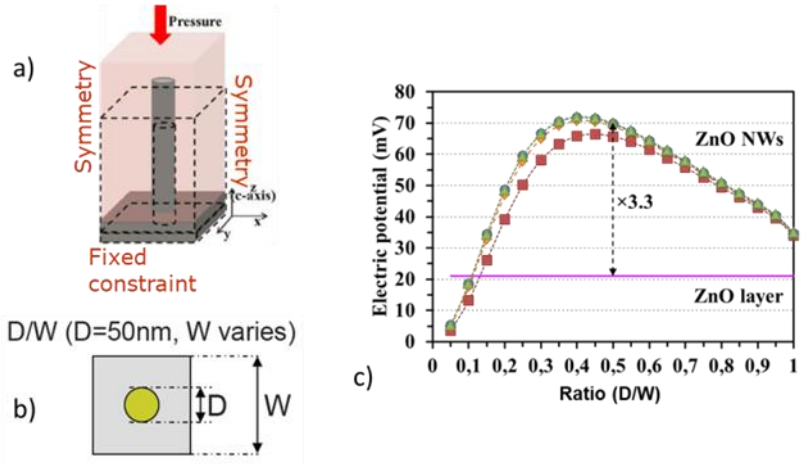

Figure 3: Simulation results of a VING device under compression (1 MPa). a) Individual cell of the device with proper boundary conditions to consider the cell surrounded by other cells. b) Definition of the NW density (top view of a single cell). c) Potential generated in function of the NW density. The NWs in the model were 50 nm wide and 600 nm long. [24]

In [25], Tao *et al.* used similar models and the same approach of considering a single cell to evaluate the device performance under bending. The device was considered as a doubly clamped plate and bent by a hydrostatic pressure of 1 kPa (Figure 4a and 4b). These boundary conditions were then transferred to the individual cell (Figure 4c). The NW density and the matrix material were evaluated in these models considering the piezoelectric properties at the nanoscale [26]. They found several ways to improve the performance which were different compared to the device evaluated under compression: i) Immerging the NWs into a hard matrix material and ii) using a higher density of NWs (Figure 4d and e). These simulations did not include the semiconductor properties on the ZnO NWs. In a later publication [27], Tao *et al.* considered not only the improved piezoelectric coefficients ZnO but also the reduced dielectric coefficients [28] at the nanoscale resulting in a further improvement of the whole device performance.

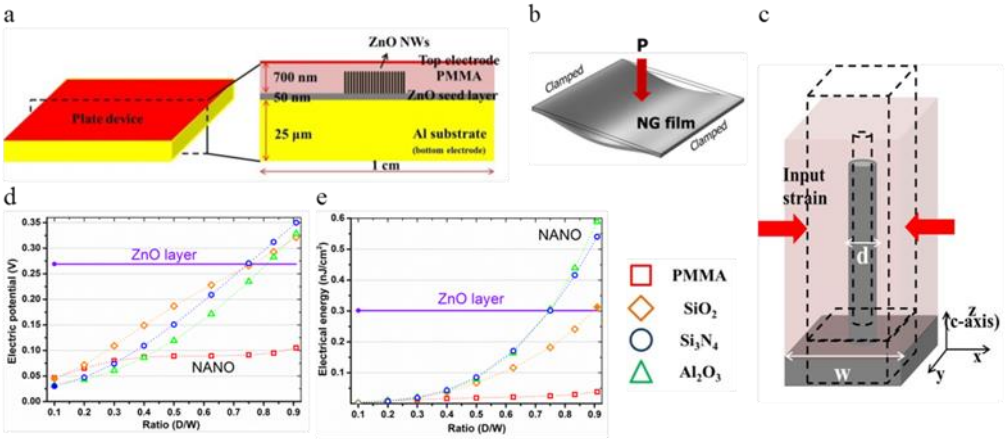

Figure 4: (a) Schematic of the cross section of the VING device. (b) Deformation of the doubly clamped device and (c) unit cell under flexion where the input strain to the plate (device) is transferred laterally to the cell. (d) Electric potential and (e) electric energy of an individual cell using different matrix materials and as a function of the NWs density. A thin ZnO layer was simulated as well as a reference. The NWs in the model were 50nm wide and 600nm long with piezoelectric properties reported at the nanoscale [25]

From a theoretical point of view, models of single piezoelectric NWs (not immerged into a matrix) including semiconductor properties and evaluated in flexion or compression lead to results where a very small voltage was generated [29, 30]. For typical doping concentrations

(~ 1×10^{17} cm^{-3}), the expected voltage is nearly reduced to zero. This is because the free carriers inside the NW screen the piezoelectric potential. The expected theoretical voltage generated from devices based in ZnO NWs is then very low. In contradiction with this theory, as mentioned above, experimental data show that the composite can actually generate decent levels of voltage.

More recently, Tao *et al.* [31] evaluated the importance of including in the models the semiconducting properties and in particular surface traps at the interface between ZnO and the dielectric matrix. Surface traps are commonly present at the surface of III-V and II-VI semiconductor compounds and are responsible of Surface Fermi Level Pinning (SFLP) [32-34]. They evaluated the VING configuration under compression and bending at a fixed medium NW density, medium density of surface traps (5×10^{11} $cm^{-2}eV^{-1}$) and then varied the doping concentration. They found that surface traps depleted the NWs allowing the generation of decent values of piezoelectric potential at typical values of doping concentration (Figure 5). In general, the composite presented better performance and for a wider range of doping concentration compared to thin films. The inclusion of surface traps and SFLP could explain experimental results reported in the literature.

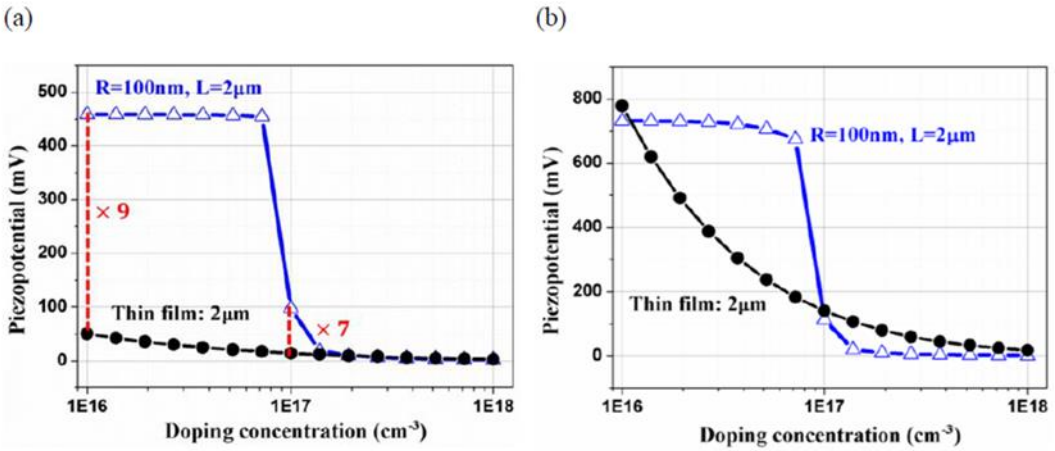

Figure 5: Comparison of the absolute value of the piezopotential generated by a VING unit cell including SFLP, with that of a ZnO thin film, where SFL can be pinned only on top interface, a) in compression mode and b) in flexion mode. The NW in the cell had a radius of 100 nm and a length of 2 μm, while the ZnO thin film was 2 μm thick. [31]

4 Regarding the Photo-mobile Polymer (PMP) suitable for this project

Besides the realization of direct conversion of light energy into mechanical work obtainable by light-induced Marangoni's effect [35, 36], based on the surface tension gradient induced by light on a fluid surface [37, 38], from decades [39] such a result is achievable by means of Photomobile Polymer films (PMPs). PMP is intended to be a film (usually, a plastic film) of which the deformations can be induced and controlled by an impinging light (in terms of its intensity, polarization state, wavelength). Substantially, PMP actuators change their shape or volume in response to light [40]. These materials have photoresponsive units [41]. The changes in physical properties of the material are related to changes in the molecular rearrangement of the single units. For example, some PMPs contain anthracene that can photodimerize under UV light. The photomechanical effects of these polymers are influenced by glass transition temperature [42]. Liquid crystal (LC) addition in these polymers can enhance their photo-response [43]. Another example is given by poly-(4-vinylpyridine)

(P4VP) which can form a supramolecular complex with various compounds orienting the functionality on side-chain polymers [44]. The polymer complex film bent toward a 310 nm light source without chemical bonding to the polymer. A photoreactive complex polymer fiber is prepared from P4VP and photoreactive carboxylic acid. The photobending effect is enhanced by introduction of a liquid crystal. The complex fibers exhibit significant photomechanical properties and can be prepared from available commercial compounds [45].

In order to give a general view on the PMP present in literature and/or commercially available it is possible to classify PMPs in three main categories:

a) PMP based on liquid crystals architecture (and generally - but not exclusively - based on azo-benzenes liquid crystals), here called LC-PMP (regarding the azobenzene based LC-PMP, here, in this document, azo-LC-PMP). [46-51] Actually, the first theorization on the use of liquid crystals in order to reach the photo-motility is to be attributed to De Gennes, 1969, [52] while the first highly performing LC-PMPs is to be attributed to the Ikeda's group [39]. The further development of such a technology brought to the realization of highly frequency oscillation LC-PMPs, [51] in particular here we remind the LC-PMP realized by the group of Tabiryan, in 2008, [51] where the oscillation frequency reached ~ 27 Hz, having a life time of ~ 2.5 hours under continuous irradiation of a laser light source; beside its relatively short life time, such a technology is to be put under our attention due to the high oscillation frequency achieved. In particular, LC-PMPs are of strong interest for the following reasons: 1) their "motion" under different wavelengths and polarization states of an impinging light is well tested and they are the most present in literature; 2) they offer a high oscillation frequency and large bending angle; 3) they are commercially available (for example, they should be available @ BEAM Engineering for Advanced Measurements Company, Winter Park, FL 32789, USA, Beamco.com, Florida, USA). 4) they should resist the immersion in water, at relatively high temperatures. Recently, this same basic structure was cross-linked to obtain high performance azo-LC-PMP fibers, capable to survive, for example, in water or compatible solvents, such as Tetrahydrofuran (THF) [53]; in this latter case, azo-LC-PMP architecture should allow, in principle, to obtain the desired film;
b) bilayered-PMP (bi-PMP): PMP based on the different expansion coefficient between layers in a bi-layered architecture, such as those based on the single-wall carbon nanotubes (SWCN) and polycarbonate or those based on graphene oxide/carbon nanotubes and PDMS [54, 55].
c) PMPs-r: PMPs based on the interfacial tension gradient between layers [56], of which the restoration (that is the restoration of the starting position/3D configuration of the PMP) should be regulated by diffusion. In this case, it is realized by using a mixture of multireticulated polymers and N-Vinyl-Pirrolidone (NVP), doped by the oxidation of phenols substitutes, by asymmetric photo-polymerization procedure.

For what concerns the azo-LC-PMP motion is the resultant of cis-trans isomerizations of the components of the film under light irradiation. In synthesis the film is generally (buy not uniquely) based on a Liquid Crystal azobenzene monomer and liquid crystal azobenzene di-acrylate (1:4). The resultant of the cis-trans isomerization of all the components produces the deformation at macroscopic level under light that is sensitive to the wavelength and polarization state of the impinging light. As an example, we report on the formula structure of the monomers used to obtain high performance azo-LC-PMP (azobenzene-based, in this case) to which are ascribable many the azo-LC-PMP:

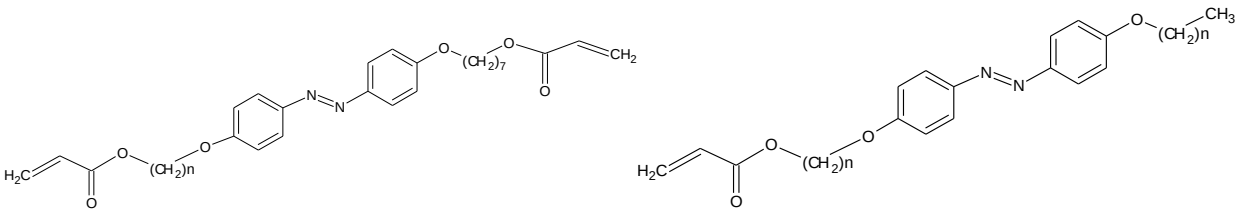

Figure 6: formula structures of the monomers for azo-LC-PMP. By changing the length of the alkyl chain of the single monomers $(CH_2)n$, the properties of the final PMPs are changing.

The properties of the different films are based on the different lengths of the alkyl chains of the monomers (as illustrated in
Figure 6).

However, in principle, the PMP polymer required for our project should be able to be deformed under light and to restore its initial position/configuration when the light is switched-off. From this point of view it is preferred a kind of PMP that doesn't require the use of different wavelengths and polarization states in order to restore its initial position or to allow the PMP motion. In this case, it is preferred to use bi-PMPs.

They can be attractive for our proposal, in particular when looking at the experiments of X. Zhang *et al.* [54], where the continuous illumination under a sun simulator gives rise to a continuous motion, as illustrated in the pictures of Figure 7.

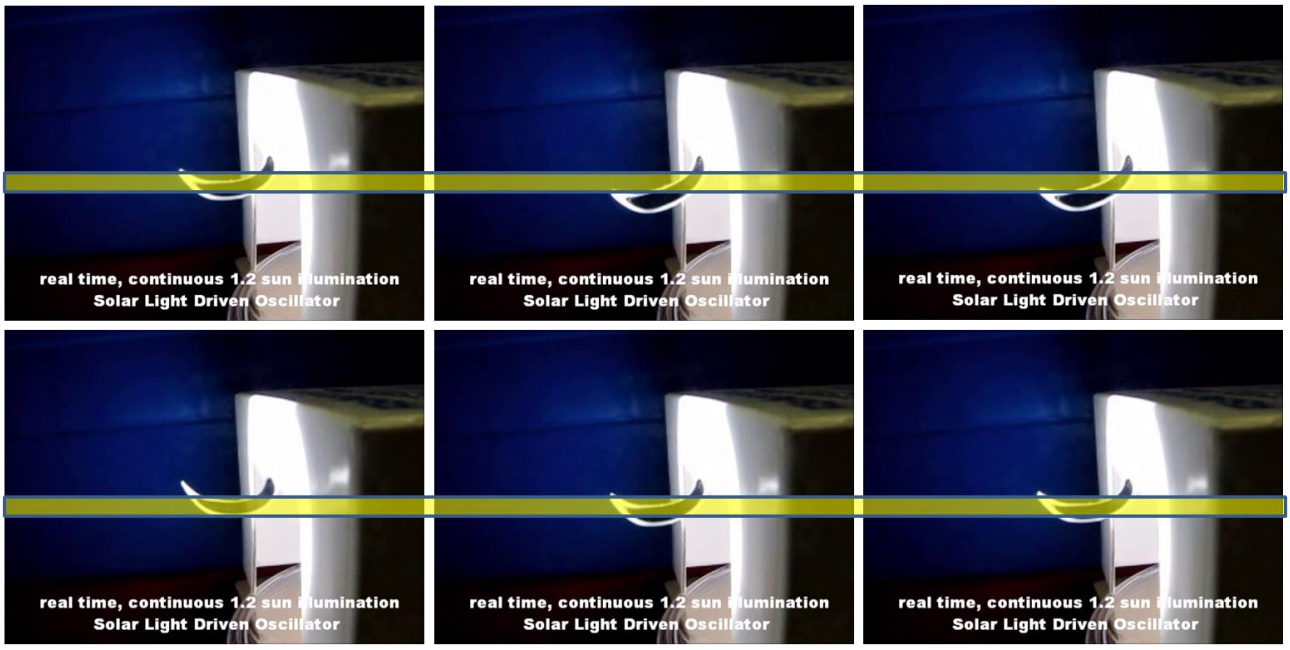

Figure 7: From left to right different frames of the video in Supporting information of X. Zhang et al. [54] regarding the solar light driven oscillator (the horizontal yellow line is added to better highlight the movement of the polymer under illumination).

In this case, the resistance under ZnO NWs fabrication procedure is still to be tested, but it should be noted that the materials offer a certain resistance to both the relatively high temperature and water.

Meanwhile, the PMP-r of which the motion is based on the interfacial tension gradient is also attractive for the same reasons. In all cases, the protection by an envelope needs to be considered.

Thus, while we should pay attention to LC-PMP (and, in particular, to azo-LC-PMPs) since they are highly performing PMPs and can be useful in order to obtain high bending, high bending rate, and are well tested in regarding to their deformation under light, we have to be care to the fact that the restoration of the PMP should be preferentially self-guided (light / no-light = motion / restoration). Furthermore, since LC-PMPs are realized by linear polymer chains, they are sensitive to solvents (in this case, we have to protect the LC-PMPs by encapsulation).

In PULSE-COM we should also realize azo-LC-PMP following the procedure steps proposed by the literature [39, 51] and in particular classic synthesis [39, 57] as comparison materials. It is worthwhile to underline that the classic synthesis for this kind of photopolymers requires many steps of reactions. The monomers for this kind of polymers are, however, also provided by companies. A further drawback to be considered is the necessity of polarized light in order to initiate their oscillations [57].

For what concerns the PMP-r films, we have to pay attention to those recently ideated and developed. [56] They are based on the photo-polymerization of organic mixtures made as follows: Multiacrylate (MA), Pirrolidone-derivative (Pd), phenol-substitutes (Ps), Lead-oxide and photo-initiators (Pi) in the UV-Vis regions. Lead oxide should be replaced, since Lead is toxic. [5] In this case, we should use different oxidation procedures: from those based on the use of organic oxidants at the required temperatures and/or in presence of Iron salts and/or Iron (II/III) oxides - that can be easily removed from the reaction environment. Regarding the sample preparation, the used mixture should be based on the following composition: MA + Pd + Ps + Pi in the UV-Vis region blended together. The final mixture is suitable to be used after keeping it in darkness overnight at room temperature under magnetic stirring in aerobic conditions. After that, the mixture is placed by capillarity between two standard microscope glasses - spaced by 200 µm using Mylar stripes - and let polymerize under a UV light. At the end of the UV exposure, a polymer layer of ~ 20-25 µm thickness is found to be glued on the top glass surface. Then, by gently removing the glasses, the film is easily peeled-off from the upper glass substrate, and it is ready to be used. Below the sequence of the production steps is reported (Figure 8).

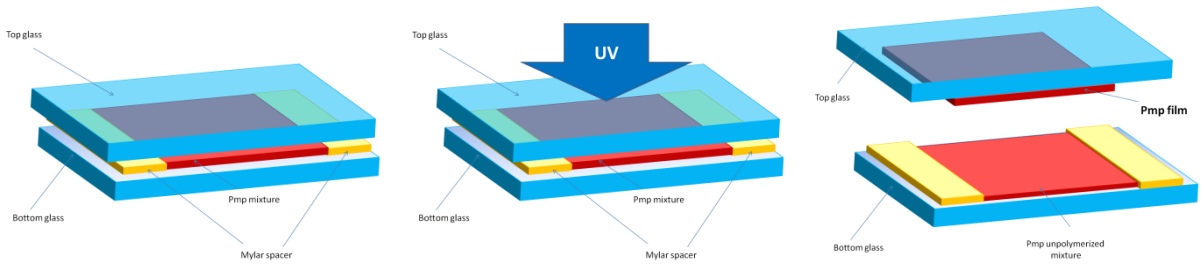

Figure 8: Scheme describing the sequence for the PMP film fabrication [56]. From left to right: the mixture is inserted by capillarity into a sandwich of glass slides (1 mm thickness) spaced by Mylar stripes (~ 200 µm thickness); the sandwich is placed under UV light for 10 minutes; at the end of irradiation the PMP-film is attached on the top glass.

Thus, the first approach should be based on the complete characterization of all the oxidation derivatives of Ps in order to find-out the basic compounds playing the crucial role in the PMP-film constitution and in its light-induced motion, and to offer higher-performances PMP-systems. In shorts, Ps are oxidized before to be dissolved in the pre-PMP mixture; Ps will be oxidized at different relative concentrations of the oxidant used in the opportune solvents (Cl-benzene solution, for example) in order not to initiate undesired oxidations. It is

to be remarked that can be used also other kinds of oxidation reactions (for example, initiated by light irradiation, or nitration and/or nitrosation, or by organic oxidants on which the Fenton-like reaction can be initiated by Fe (II/III)-oxides and/or salts, and easily removable from the reaction environment). The derivative products of Ps oxidation will be separated by preparative thin layer chromatography (tlc) and analyzed by Mass spectroscopy, NMR, IR, Raman, SERS and LSPR spectroscopies. It is to be underlined, at this stage, that the oxidation of Ps could have important intermediates such as stable free radical cations. We should assess the importance of free radicals cations in the system by using stable free radicals cations in the pre-polymerized PMP mixture. Furthermore, each product of the phenol-derivative oxidation should be separately and in combination used in the pre-polymerized PMP-mixture in order to assess its functionality and role in the light-induced motion of the PMP-film. The MA used should be based on multifunctional acrylates (di, tri, tetra) and/or multi-epoxides and on their combinations. The investigation on the effects of the oxidated form of Ps on the Pd will be also analyzed, by all the techniques mentioned for oligomers / polymers characterization. The final PMP film, obtained after UV illumination, will be analyzed by many different techniques all related to the polymer chemistry. ATR-FTIR and Scanning Electron Microscopy (SEM) measurements will help to understand the structure of the PMP-film before and after gold coating. The PMP-motion characterization is easily performed by simply modulating the illumination on the PMP-film. Preliminary results confirm that the motion is inducible by a white lamp of an optical microscope, but also by lasers at different wavelengths (λ = 405 nm; λ = 532 nm; λ = 785 nm); the recording of the motion by a CCD camera will allow to exactly calculate the mechanical stress of the PMP-film and its response under light illumination. The relaxation time is also important in establishing the efficiency of the PMP light-driven motility.

5 Regarding plasmonics, photonic crystals and metasurfaces suitable for this project

From the experimental measurements carried out in literature, it is clear that the performance of the PMP film, regardless of the mechanisms that regulate its motion, are also closely connected with the absorbed light power [51]. In order to increase the absorption of PMPs and to extend it to Near Infra-Red (NIR) and Short Wave Infra-Red (SWIR) regions, one solution is to implement different optical systems in PMPs architectures.
Optical systems suitable for the project are based on: a) ultrathin metallic layer deposition on the PMP surface (Paragraph 5.1); b) photonic crystals and metasurfaces nestled on the PMP surface (Paragraph 5.2); c) nanoparticles insertion in PMP pre-polymerized mixture (Paragraph 5.3).
These strategies based on different optical mechanisms produce different phenomena that could be employed to better exploit the incident radiation.
In particular, as far as ultrathin metallic layer could exploit the plasmonic resonance that permit the absorption at particular wavelengths that otherwise would not be possible. Because of this absorption, it is possible to realize a thermal gradient that could support the bending of PMP films composed by a bilayer (such as PMP-r).
In case of employing photonic crystals and metasurfaces it would be possible to use the diffraction mechanism to increase the photon-PMP interaction times (also known as dwelling-times) increasing the probability to trap the light with different angles inside the film trying to enhance the absorption of the PMP itself.
In the last case, the exploited mechanism will be the diffusion effect due to the presence of the nanoparticles that will again enhance the light trapped inside the PMP film and the

consequent absorption. If the particles are metallic, it could be possible to exploit also in this case the plasmonic mechanism.
In case the function is opto-thermal rather than light engineering, the requirement to the polymer would be high thermal expansion rather than photo-responsivity but in both case we will have an advantage in the PMP bending effect and the consequent transduced potential difference at the PZL electrodes.
In the following table, we summarized the proposed strategies and related mechanisms:

Optical elements	Effect	Interest
Ultrathin metallic layer	Plasmonic resonance that permit the absorption at particular wavelengths.	Possibility to realize a thermal gradient that could support the bending of PMP films composed by a bilayer
Photonic crystals and metasurfaces	Diffraction mechanism	Increase the photon-PMP interaction times (also known as dwelling-times) increasing the probability to trap the light with different angles inside the PMP film
Nanoparticles	Diffusion	The scattered light due to the presence of the nanoparticles could enhance the light trapped inside the PMP film and the consequent absorption. If the particles are metallic, it could be possible to exploit also the plasmonic mechanism.

5.1 Regarding ultrathin metallic layer deposition

Ultrathin metallic film processed onto the PMP surface, would result in a much greater absorption by the PMP/film system. As far as with the use of ultrathin metallic layer, in fact, we could exploit the plasmonic resonance that permit the absorption at particular range of wavelengths that otherwise would not be possible. Light-induced heat generation in materials occurs due to dissipation of heat from oscillation of free electrons on a metallic lattice surface – the surface plasmon resonance (SPR) driven by resonant wavelength of light [58]. Gold (Au) and silver (Ag) nanoparticles can have a very good thermal conversion coefficient. For example, the SPR of Au nanospheres can be tuned within the visible range by varying the wall thickness and the distances between them. Besides gold (Au), silver (Ag) has been known as potentially the best plasmonic material with the naturally lowest ohmic losses at optical frequencies. Despite the apparent simplicity of a single ultra-thin film deposition, the accurate measurements of film thickness for final characterization, could be rather difficult. The Ag ultra-thin film must be processed using a very low rate of deposition, in any case under 0.01 nm/sec, in vacuum conditions assisted with pure Argon (99.99%) gas flow at 20 s.c.cm – 30 s.c.cm. The working vacuum must be optimized according to specificity of vacuum chosen system. The candidate equipment is electron beam evaporation system, magnetron sputtering, ion beam sputtering with ion beam assisted or another complex system. The nucleation of ultra-thin Ag film can be observed by Atomic Force Microscopy (AFM) measurements. Nucleation of Ag film, deposited by magnetron sputtering, resulting like nanostructure can be significantly influenced by an ultra-thin silver-oxide interlayer [59]. We have already used ultra-thin Ag films with thicknesses between

3 nm up to 25 nm and the refractive index measurements were given values in the proximity of zero within spectral range 400 nm to 700 nm. Samples coated on fused silica and borosilicate glasses, AFM explored, have appeared like self-organized micro-structures [60]. Plasmonic materials, like Au and Ag, are used in a variety of devices and are especially important in the recent boom of metamaterials. J.B. Pendry [61] demonstrates that a slab of negative refractive index material, like Ag ultra-thin film, has the power to focus all Fourier components of 2D images, even those that do not propagate in a radiative manner. Simulations show that a version of the lens operating at the frequency of visible light can be realized in the form of a thin slab of silver. The applications of plasmonic materials, the near-field super lens/flat-lens and the far-field hyper lens, have attracted a great deal of both theoretical and experimental research interest. Ag is the most often used metal material in flat lenses and plasmonic applications since Ag exhibits the lowest on-resonance loss of any natural noble metal at optical frequencies [62]. In shorts, combining the properties of ultra-thin silver (Ag) films to attain the refractive index towards zero and plasmonic behavior at optical wavelength, it is reasonable to design experiments, as intermediary technological phase, with Ag deposition on the surface of the PMPs to obtain new functionalities in the PMP layer. It is worthwhile to underline that with this kind of mechanism, it is possible to realize a thermal gradient (opto-thermal effect) that could better support the bending of PMP films composed by a bilayer (such as PMP-r).

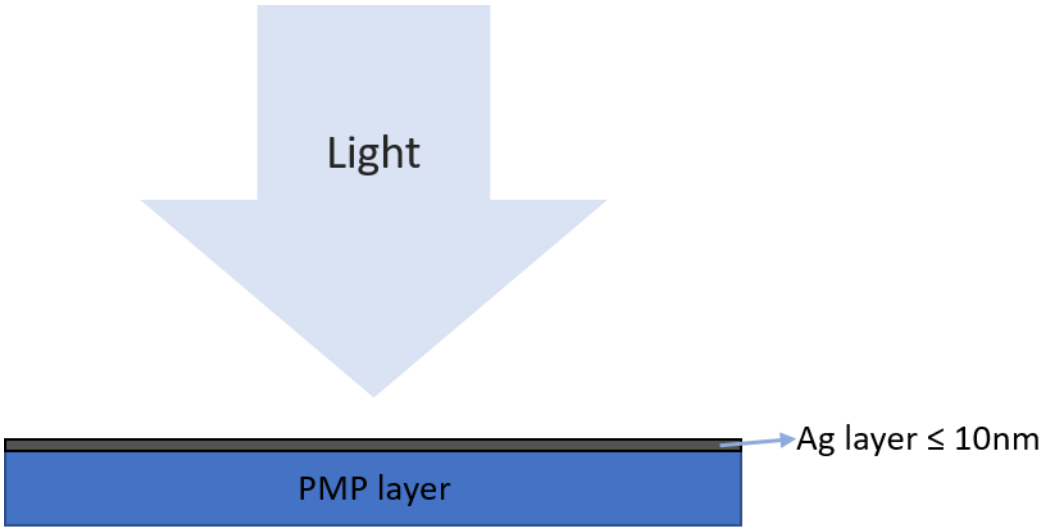

Figure 9: Sketch of the ultra thin Ag-layer deposited on the PMP surface. The thickness of the layer is in the range of 10 nm.

5.2 Regarding Photonic crystals and metamaterials/metasurfaces

Another option to add new functionalities to the PMP material is by the use of photonic crystals and metasurfaces. In case of employing photonic crystals and more complex structures such as metasurfaces it would be possible to use the diffraction mechanism to trap the light with different angles inside the PMP film trying to enhance the absorption of the PMP itself.
Photonic Crystals (PC) are highly ordered materials which possess a periodically dielectric constant, with periods on visible light wavelengths (380 - 750 nm). Periodicity influences electromagnetic waves in the material because of Bragg reflections. It results a photonic band gap (PBG), a band where light propagation in the photonic crystal is forbidden (the optical analogue of electronic band gaps in semiconductors). A complete PGB occurs when a wavelength is forbidden for every polarization and direction [62]. Since Yablonovitch [63]

and John [64] demonstrated the possibility of a photonic band gap in such periodic structures, serious effort was made by the scientists to develop materials with complete photonic band gaps in several optical regimes and in particular in the visible region [65]. Complete photonic band gap materials could be used to produce waveguides, laser resonant cavities, laser mirrors or to inhibit spontaneous emission [66]. Photonic crystals are usually produced by nanolithography and self-assembly of colloidal crystals. A different approach consists in crystallization of a colloidal suspension of monodisperse spheres of silica, ZnO, chalcogenide or organics forming a three-dimensional structure with 24% air, called colloidal crystal or opal [67, 68], A complete PBG can be easily obtained in materials with inverse opal structures, formed by air spheres in materials with high refractive indices (e.g. Si n = 3.5 or Ge n = 4.5) [67]. The opals and inverse opals can be used in solar energy conversion or LEDs. For our aims an opal or inverse-opal structure could be formed on top of PMP leading to new or enhanced properties for energy-harvesting, sensing, laser mirrors or resonant cavities. As an example of photonic crystal realization we report Vita F. *et al.* work [69], in Figure 10, where an interference pattern of light is used (instead of a simple illumination by UV/Vis lamp) and the photo-polymerization could give rise to a refractive index distribution corresponding to maxima and minima of the interference intensities.

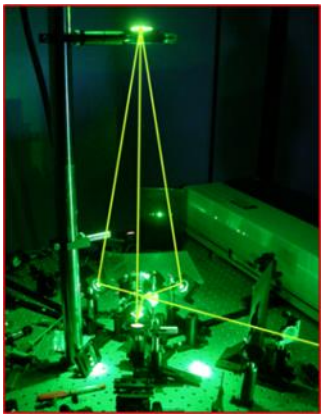

Figure 10: Example of fabrication of bi-dimensional (right) photonic crystals by using an interference pattern of light [69].Photonic crystals can be based on different geometries (for example, on octupolar metasurfaces geometry, of which the structure is mainly constituted by the periodic and aperiodic repetition of triangular units [70]). The final geometry should involve a fractal configuration.

Metamaterials (MMs) are materials of which the properties are obtained from their structures and designed unit cells (meta-atoms) [71] and not from the properties of their constitutive materials. Also the optical PCs properties are defined by their structures. Metasurfaces (or metafilms) are 2D MMs. Like MMs, their response can be characterised by their electrical and magnetic polarizabilities. MMs control the propagation of light due to their permittivity and permeability values. [72]
MMs and metasurfaces are then engineered materials able to manipulate electromagnetic waves at variable frequency regimes, ranging from UV–visible to infrared (IR) to terahertz (THz).
Examples of MMs and metasurfaces properties and applications are: negative, near-zero, indefinite permittivity or permeability indices; backward waves and backward phase matching in nonlinear optics; imaging below the diffraction limit; perfect absorption [71-76].

5.2.1 Regarding nanostructures implantation on the PMP-film surface

While the PMPs related to categories (a) LC-PMP and (b) bi-PMP should be still tested in this context, at present, we have encouraging preliminary results supporting the possibility to successfully obtain the implantation of plasmonic nano-structured crystal substrates on

the PMP-film surface. By taking into account a multi-acrylate based PMP-r film, due to the high shrinkage under photo-polymerization, [77] we observed that the photo-polymerization of the PMP-mixture in contact with previously fabricated PCs or MMs, allows the extraction of gold from sub-micro-/nano-pillars. The confirmation of the presence of the PCs or Metacrystals on the PMP-film surface should be obtained by investigations with many techniques (AFM, SEM, Dark/Bright-field microscopy Optical Measurements, Optical Far Field Scattering measurements, Localized Surface Plasmon Resonance (LSPR) measurements, Surface Enhanced Raman Scattering (SERS) measurements). At the moment, Dark-field (DF) observations, Optical Far Field scattering measurements and LSPR measurements indicate that PMP-film can actually support PCs or plasmonic metacrystals on its surface. Figure 11 reports the experimental set-up for an LSPR analysis. We have preliminary results indicating that implantation of the plasmonic metacrystal on the PMP-film surface is possible and measurable.

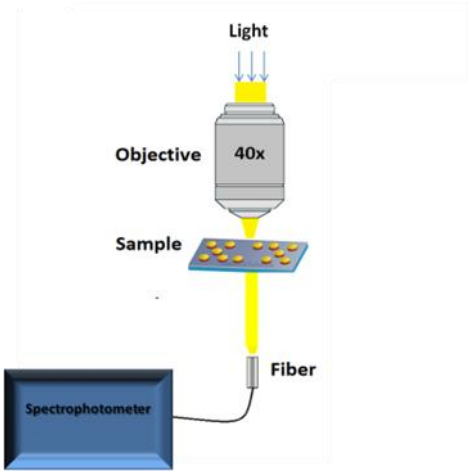

Figure 11: Experimental set-up for LSPR analysis [78].

The possibility for obtaining SERS signals from metacrystals placed at the PMP-film surface is still to be verified but, if confirmed, will expand the capabilities of our system.

5.3 Nanoparticles insertion in PMP

The use of plasmonic nanoparticles could allow from one side to increase the robustness of the system, while from the other side to modulate its absorbance properties, in order to expand the absorption range of the PMP-PZL.
In particular, in this case, the exploited mechanism will be the diffusion effect due to the presence of the nanoparticles that will again enhance the light trapped inside the PMP film and the consequent absorption.
Furthermore, if the particles are metallic, it could be possible to exploit also the plasmonic mechanism adding an opto-thermal effect to a light scattering effect. In both case we will have an advantage in the PMP bending effect, and in the reaction times with the consequent advantage in the transduction of the potential difference at the PZL electrodes for a full PMP/PZL device.

6 Regarding the encapsulation/protection of the system

The choice for flexible encapsulation technique is very critical to accomplish our aim. Flexible substrates and the right encapsulation are fundamental in many fields of organic electronics, e-paper's and e-ink's development. Many different types of materials are nowadays under investigation, including glasses, polymer films and metallic foils. In this

particular case we have to consider reports of studies of polymer films as flexible substrates for polymer light emitting diodes (PLEDs) or organic photovoltaic (OPV) technologies and their encapsulation procedures. Usually, the selected polymer substrates are thermoplastic semi-crystalline polymers like Polyethylene Terephtalate (PET) and Polyehtylene Naphtalate (PEN), in our case - obviously - our substrate will be the PMP-film. The encapsulation barrier technology is traditionally essential for preventing the degradation of flexible devices. For OLEDs and OPVs the design objectives of the encapsulation barrier depend on the required Water Vapor Trasmission Rate (WVTR) and lifetime of the device in actual industrial products, in our case, for the encapsulation process, we must pay particular attention to the PZL implementation constraints to better protect the PMP film. Traditionally, three types of encapsulation barrier technology have been used for devices: glass lid encapsulation, barrier foil encapsulation, and thin-film encapsulation (TFE). Above all, TFE is the most promising encapsulation technology for devices because it is flexible and easy to apply to any device and it can be applied easily to flexible, rollable, and foldable devices. Moreover, TFE does not require the use of adhesive. Some disadvantages of this technology, however, are the potential damage of the device through direct deposition and limited processing conditions. [79-81]

Our needs are certainly less stringent than those relating to electronic devices. In our case a flexible encapsulation is required and this can be obtained simply by using the TFE procedures. We should focus on polymers used as capping layers.

The encapsulation materials, surely, should have be low cost and should be easy to deposit. But more important, the selected material has to be transparent, with appropriate glass transition temperature (Tg) which is dependent on the chain flexibility, a complex function of several factors such as chemical structure, molecular mass, presence of cristallinity or additives. Above glass transition temperature the polymer mechanically varies from being rigid and brittle and becomes tough and leathery. The maximum exposure temperatures on encapsulation material and the effect on the mechanical behaviour of the material should be known. The light transmission through the encapsulation materials is also important to understand how it will affect the device performance and this is much more important for the PMP films.

Suitable polymer materials for encapsulation process already used for flexible electronics devices are: ethylene vinyl acetate copolymer (EVA) [82, 83], polyvinyl butyral (PVB) [84], other organic materials [85, 86], and Polydimethylsiloxane (PDMS).

Probably the most appropriate material for PMP films is the Polydimethylsiloxane (PDMS), benefiting from a low cost, ease of moulding, biocompatibility, chemical stability and transparency, has been widely used in fabrication and encapsulation processes for electronic devices. [87-92] What's more, the excellent ductility of PDMS gives it potential in the extensive application of flexible electronics. Importantly, PDMS solution is water-free making it a perfect choice to package the PMP film because it resists to high-temperature (up to 350°C) [93], has good mechanical properties and, no less important, it has excellent transparency [94, 95].

7 Conclusions

The state of the art for structures and devices that can be employed in PULSE-COM is definitely very wide and in this report we tried to present an overview of papers from literature

which address to these issues. We reported more in details on materials and techniques which can be explored during the project.
We reported on the possibility of integrating piezo-electric devices on flexible substrates considering all the possible architecture and materials reported in literature. We considered also organic piezo materials (PVDF, PVDF-TrF etc.) and based on different piezo composites ($BaTiO_3$ and ZnO nanowires). We discussed the possibility to use different substrates and in particular to use also extremely flexible one such as PDMS with a very low Young's modulus.
We reported on the use of different PMP materials and architectures (LC-PMPs / azo-LC-PMPs, bi-PMPs and PMPs-r) and how to improve their functionalities with plasmonic nanomaterials and engineered nanostructures.
Finally, we reported on possible protection/encapsulation system configurations to protect the PMP substrate.

As a first approach, we should focalize on ZnO-nanowire-based PZLs (ZnO-NW-PZL), on PMPs-r and PDMS (for encapsulation). We should make tests of integration of ZnO-NW-PZL on each category of PMP and encapsulate/protect when needed.

References

[1] D. Grbovic, S. Obswald "Bi-material Micro-Electro-Mechanical System (MEMS) Solar Power Generator", PATENT Number: US 8,525,393 B1

[2] C. Dagdeviren, P. Joe, O. L.Tuzman, Kwi-Il Park, K. Jae Lee, Y. Shi, Y. Huangh, J. A. Rogers "Recent progress in flexible and stretchable piezoelectric devices for mechanical energy harvesting, sensing and actuation", Extreme Mechanics Letters, 2016, 9, 269–281.

[3] Y. Qi, J. Kim, T. D. Nguyen, B. Lisko, P. K. Purohit, M. C. McAlpine "Enhanced piezoelectricity and stretchability in energy harvesting devices fabricated from buckled PZT ribbons", Nano Letters, 2011, 11, 3, 1331-1336

[4] S. Xu, Y. W. Yeh, G. Poirier, M. C. McAlpine, R. A. Register, N. Yao "Flexible piezoelectric PMN–PT nanowire-based nanocomposite and device", Nano letters, 2013, 13(6), 2393-2398.

[5] http://data.europa.eu/eli/dir/2011/65/2014-01-29

[6] Z. H. Liu, C. T. Pan, L. W. Lin, J. C. Huang, Z. Y. Ou "Direct-write PVDF nonwoven fiber fabric energy harvesters via the hollow cylindrical near-field electrospinning process", Smart Materials and Structures, 2013, 23(2), 025003.

[7] T. Sharma, S. S. Je, B. Gill, J. X. Zhang "Patterning piezoelectric thin film PVDF–TrFE based pressure sensor for catheter application. Sensors and Actuators A: Physical, 2012, 177, 87-92.

[8] K. I. Park, S. B. Bae, S. H. Yang, H. I. Lee, K. Lee, S. J. Lee "Lead-free $BaTiO_3$ nanowires-based flexible nanocomposite generator", Nanoscale, 2014, 6, 15, 8962-8968

[9] M. Akiyama, Y. Morofuji, T. Kamohara, K. Nishikubo, M. Tsubai, O. Fukuda, N. Ueno "Flexible piezoelectric pressure sensors using oriented aluminum nitride thin films prepared on polyethylene terephthalate films", Journal of Applied Physics, 2006, 100, 11, 114318.

[10] S. Mukhopadhyay, M. E. E. Alahi, "Smart nitrate sensors", Springer Ed., 2019.

[11] S. Lee, R. Hinchet, Y. Lee, Y. Yang, Z. H. Lin, G. Ardila, L. Montes, M. Mouis, Z. L. Wang "Ultrathin nanogenerators as self-powered/active skin sensors for tracking eye ball motion" Advanced Functional Materials, 2014, 24, 8, 1163-1168.

[12] Y. Hu, Y. Zhang, C. Xu, G. Zhu, Z. L. Wang "High-output nanogenerator by rational unipolar assembly of conical nanowires and its application for driving a small liquid crystal display", Nano letters, 2010, 10, 12, 5025-5031.

[13] M. H. Zhao, Z. L. Wang, S. X. Mao "Piezoelectric characterization of individual zinc oxide nanobelt probed by piezoresponse force microscope", Nano Letters, 2004, 4, 4, 587-590.

[14] Z. L. Wang and W. Wu, "Nanotechnology-enabled energy harvesting for self-powered micro-/nanosystems", Angewandte Chemie International Edition, 2012 51, 47, 11700-11721.

[15] S. Xu, Y. Qin, C. Xu, Y. Wei, R. Yang, Z. L. Wang "Self-powered nanowire devices", Nature Nanotechnology, 2010, 5, 366–373.

[16] Y. Hu, Y. Zhang, C. Xu, L. Lin, R. L. Snyder, Z. L. Wang "Self-Powered System with Wireless Data Transmission", Nano Letters, 2011, 11, 2572-2577.

[17] A. S. Dahiya, F. Morini, S. Boubenia, K. Nadaud, D. Alquier, G. Poulin-Vittrant "Organic/Inorganic Hybrid Stretchable Piezoelectric Nanogenerators for Self-Powered Wearable Electronics", Advanced Materials Technologies, 2018, 3, 2, 1700249.

[18] M. Choi, G. Murillo, S. Hwang, J. W. Kim, J. H. Jung, C. Y. Chen, M. Lee "Mechanical and electrical characterization of PVDF-ZnO hybrid structure for application to nanogenerator", Nano Energy, 2017, 33, 462-468.

[19] Y. Hu, L. Lin, Y. Zhang, Z. L. Wang "Replacing a battery by a nanogenerator with 20 V output", Advanced Materials, 2012, 24, 1, 110-114.

[20] J. J. Briscoe, M. Stewart, M. Vopson, M. Cain, P. M. Weaver, S. Dunn "Nanostructured p-n junctions for kinetic-to-electrical energy conversion", Advanced Energy Materials, 2012, 2, 10, 1261-1268; b)

[21] J. J. Briscoe and S. Dunn, "Piezoelectric nanogenerators – a review of nanostructured piezoelectric energy harvesters", Nano Energy, 2015, 14, 15-29.

[22] O. Graton, G. Poulin-Vittrant, A. S. Dahiya, N. Camara, L. P. T. H. Hue, M. Lethiecq "Equivalent circuit model of a nanogenerator based on a piezoelectric nanowire–polymer composite", Physica Status Solidi (RRL)–Rapid Research Letters, 2013, 7, 10, 915-918.

[23] R. Hinchet, S. Lee, G. Ardila, L. Montes, M. Mouis, Z. L. Wang "Design and guideline rules for the performance improvement of vertically integrated nanogenerator," Journal of Energy and Power Engineering, 2013, 7, 9, 1816.

[24] R. Hinchet, S. Lee, G. Ardila, L. Montès, M. Mouis, Z. L. Wang "Performance optimization of vertical nanowire-based piezoelectric nanogenerators," Advanced Functional Materials, 2014, 24, 7, 971-977.

[25] R. Tao, G. Ardila, L. Montès, M. Mouis "Modeling of semiconducting piezoelectric nanowires for mechanical energy harvesting and mechanical sensing", Nano Energy, 2015, 14, 62-76.

[26] R. Hinchet, J. Ferreira, J. Keraudy, G. Ardila, E. Pauliac-Vaujour, M. Mouis, L. Montes "Scaling rules of piezoelectric nanowires in view of sensor and energy harvester integration", International Electron Devices Meeting (IEDM), San Francisco, USA, 2012, December.

[27] R. Tao, G. Ardila, R. Hinchet, A. Michard, L. Montès, M. Mouis "Will composite nanomaterials replace piezoelectric thin films for energy transduction applications?",

Future Trends in Microelectronics: Journey into the Unknown, 2016, Wiley, John & Sons, Inc.

[28] Y. Yang, W. Guo, X. Wang, Z. Wang, J. Qi, Y. Zhang "Size dependence of dielectric constant in a single pencil-like ZnO nanowire" Nano letters, 2012, 12, 4, 1919-1922.

[29] Y. Gao and Z. L. Wang "Equilibrium potential of free charge carriers in a bent piezoelectric semiconductive nanowire" Nano letters, 2009, 9, 3, 1103-1110.

[30] G. Romano, G. Mantini, A. Di Carlo, A. D'Amico, C. Falconi, Z. L. Wang "Piezoelectric potential in vertically aligned nanowires for high output nanogenerators" Nanotechnology, 2011, 22, 46, 465401.

[31] R. Tao, M. Mouis and G. Ardila, "Unveiling the Influence of Surface Fermi Level Pinning on the Piezoelectric Response of Semiconducting Nanowires," Advanced Electronic Materials, 2018, 4, 1, 1700299.

[32] V. Chakrapani, C. Pendyala, K. Kash, A. B. Anderson, M. K. Sunkara, J. C. Angus "Electrochemical pinning of the Fermi level: mediation of photoluminescence from gallium nitride and zinc oxide" Journal of the American Chemical Society, 2008, 130, 39, 12944-12952.

[33] H. Lüth, "Collective Phenomena at Interfaces: Superconductivity and Ferromagnetism", Solid Surfaces, Interfaces and Thin Films, Berlin, Heidelberg, Springer, 2010, 435-515.

[34] M. H. M. Van Weert, O. Wunnicke, A. L. Roest, T. J. Eijkemans, A. Yu Silov, J. E. M. Haverkort and E. P. A. M. Bakkers, "Large redshift in photoluminescence of p-doped InP nanowires induced by Fermi-level pinning", Applied Physics Letters, 2006, 88, 4, 043109.

[35] Carlo Marangoni "Sul principio della viscosita' superficiale dei liquidi stabilito dal Sig. J. Plateau", Nuovo Cimento, 1871, Ser. 2, 5/6, 239.

[36] David Okawa, Stefan J. Pastine, Alex Zettl, Jean M. J. Fréchet, "Surface Tension Mediated Conversion of Light to Work", Journal of the American Chemical Society, 2009, 131, 15, 5396–5398.

[37] D. E. Lucchetta, F. Simoni, L. Nucara, R. Castagna, "Controlled-motion of floating macro-objects induced by light", AIP Advances, 2015, 5, 077147.

[38] D. E. Lucchetta, R. Castagna, F. Simoni, "Light-Actuated Contactless Macro Motors Exploiting the Bénard–Marangoni Convection", Optics Express, 2018, 27, 10, 13574-13580.

[39] Y. Yu, M. Nakano, T. Ikeda "Directed bending of a polymer film by light", Nature, 2003, 425, 145.

[40] M. Yamada, M. Kondo, J. Mamiya, Y. Yu, M. Kinoshita, C. J. Barrett, T. Ikeda "Photomobile polymer materials: towards light-driven plastic motors", Angewandte Chemie International Edition, 2008, 47, 4986–4988.

[41] J. He, Y. Zhao, Y. Zhao "Photoinduced bending of a coumarin-containing supramolecular polymer", Soft Matter, 2009, 5, 308–310.

[42] M. Kondo, T. Matsuda, R. Fukae, N. Kawatsuki "Photoinduced deformation of polymer fibers with anthracene side groups", Chemistry Letters, 2010, 39, 234–235.

[43] M. Kondo, M. Takemoto, T. Matsuda, R. Fukae, N. Kawatsuki "Preparation and macroscopic deformation of liquid-crystalline polymer fibers crosslinked with anthracene side chains", Molecular Crystal Liquid Crystal, 2011, 550, 98–104.

[44] J., Gao, Y., He, F., Liu, X., Zhang, Z., Wang, X. Wang "Azobenzene-containing supramolecular side-chain polymer films for laser-induced surface relief gratings", Chemistry of Materials, 2007, 19, 3877–3881.

[45] M., Kondo, M., Takemoto, R., Fukae, N. Kawatsuki, "Photomobile polymers from commercially available compounds: photoinduced deformation of side-chain polymers containing hydrogen-bonded photoreactive compounds", Polymer Journal, 2012, 44, 410-414.

[46] T. Ube and T. Ikeda "Photomobile polymer materials with crosslinked liquid-crystalline structures: molecular design, fabrication, and functions", Angewandte Chemie International Edition 2014, 53, 10290-9.

[47] J.-I. Mamiya, A. Kuriyama, N. Yokota, M. Yamada, T. Ikeda "Photomobile Polymer Materials: Photoresponsive Behavior of Cross-Linked Liquid-Crystalline Polymers with Mesomorphic Diarylethenes", Chemistry - A European Journal, 2015, 21, 3174-3177.

[48] T. Ube, K. Takadoa, T. Ikeda, Photomobile materials wih interpenetrating polymer network composed of liquid crystalline and amorphous polymers, Journal of Materials Chemistry C, 2015, 3, 8006-8009

[49] T. Ube, T. Ikeda "Photomobile Polymer Materials with Complex 3D Deformation, Continuous Motions, Self-Regulation, and Enhanced Processability", Advanced Optical Materials, 2019, 7, 16, 1900380.

[50] T. Ikeda, T. Ube "Photomobile polymer materials: from nano to macro", Materials Today, 2011, 14, 480-487.

[51] T.J. White, N. V. Tabiryan, S. V. Serak, R. A. Vaia, T. J. Bunning "A high frequency photodriven polymer oscillator", Soft Matter, 2008, 4(9), 1796-1798.

[52] P. G. De Gennes "Possibilites offertes par la reticulation de polymeres en presence d'un cristal liquide", Physical Review Letters, 1969, 28A, 725-726.

[53] Z. Cheng, S. Ma, Y. Zhang, S. Huang, Y. Chen, H. Yu "Photomechanical Motion of Liquid-Crystalline Fibers Bending Away from a Light Source", Macromolecules, 2017, 50, 21, 8317-8324.

[54] X. Zhang, Z. Yu, C. Wang, D. Zarrouk, J.-W. T. Seo, J. C. Cheng, A. D. Buchan, K. Takei, Y. Zhao, J. W. Ager, J. Zhang, M. Hettick, M. C. Hersam, A. P. Pisano, R. S. Fearingl, A. Javey "Photoactuators and motors based on carbon nanotubes with selective chirality distributions", Nature Communications, 2014, 5, 2983.

[55] Y. Hu, G. Wu, T. Lan, J. Zhao, Y. Liu, W. Chen "A Graphene-Based Bimorph Structure for Design of High Performance Photoactuators", Adv. Mater. 2015, 27, 7867-7873.

[56] R. Castagna, L. Nucara, F. Simoni, L. Greci, M. Rippa, L. Petti, D. E. Lucchetta, "An Unconventional Approach to Photomobile Composite Polymer Films", Advanced Materials, 2017, 29, 1604800.

[57] H. Koerner, T. J. White, N. V. Tabiryan, T. J. Bunning, R. A. Vaia "Photogenerating work from polymers", Materials Today, 2008, 11, 7–8, 34-42.

[58] A. S. Kuenstler, R. C. Hayward “Light-induced shape morphing on thin films”, Current Opinion in Colloid & Interface Science 40 (2019) 70-86.

[59] J. Bulír, M. Novotný, A. Lynnykova, J. Lančok, M. Bodnár, M. Škereň "Preparation of nanostructured ultrathin silver layer", 2010, Proc. SPIE 7766, Nanostructured Thin Films III, 77660Q.

[60] R. Malureanu and A. Lavrinenko, "Ultra-thin films for plasmonics: a technology overview", Nanotechnology Review, 2015, 4 (3), 259-275.

[61] J. B. Pendry "Negative refraction make a perfect lens", Physical Review Letters, 2000, 85, 18, 3966-3969.

[62] W. Chen, M. D. Thoreson, S. Ishii, A. V. Kildishev, V. M. Shalaev "Ultra-thin ultra-smooth and low-loss silver films on a germanium wetting layer", Optics Express, 2010, 18, 5, 5124-5134.

[63] J.D. Joannopoulos, R.D. D Meade, Joshua N. Winn "Photonic Crystals: Molding the Flow of Light", Princeton University Press, 1995, Princeton, USA.

[64] E. Yablonovitch "Inhibited Spontaneous Emission in Solid-State Physics and Electronics", Physical Review Letters, 1987, 58, 2059.

[64] S. John "Strong localization of photons in certain disordered dielectric superlattices", Physical Review Letters, 1987, 58, 2486.

[65] V.L. Colvin "From Opals to Optics: Colloidal Photonic Crystals", Materials Research Society Bulletin, 2001, 26, 637.

[66] L. Bechger, P. Lodahl, W.L. Vos "Directional Fluorescence Spectra of Laser Dye in Opal and Inverse Opal Photonic Crystals", Journal of Physical Chemistry B, 2005, 109, 9980-9988.

[67] G. I.N. Waterhouse, M.R. Waterland "Opal and inverse opal photonic crystals: Fabrication and characterization", Polyhedron, 2007, 26, 356–368.

[68] S. Kedia, R. Vijaya, A.K. Ray, S. Sinha "Photonic stop band effect in ZnO inverse photonic crystal", Optical Materials, 2011, 33, 466–474; T. Kohoutek, J. Orava, T. Sawada, H. Fudouzi "Inverse opal photonic crystal of chalcogenide glass by solution processing", Journal of Colloid and Interface Science 2011, 353, 454–458.

[69] F. Vita, D. E. Lucchetta, R. Castagna, L. Criante, F. Simoni "Large-area photonic structures in freestanding films", Applied Physics Letters, 2007, 91, 103114.

[70] M. Rippa, R. Castagna, M. Pannico, P. Musto, G. Borriello, R. Paradiso, G.Galiero, S. Bolletti Censi, J. Zhou, J. Zyss, L. Petti "Octupolar Metastructures for a Highly Sensitive, Rapid, and Reproducible Phage-Based Detection of Bacterial Pathogens by Surface-Enhanced Raman Scattering", American Chemical Society Sensors 2017, 2, 7, 947-954

[71] J. Sun, N.M. Litchinitser, "Metamaterials", Chapter 9, Fundamentals and Applications of Nanophotonics, Elsevier Ltd., 2016, 253-307.

[72] S. S. Bukhari, J. Yiannis, Vardaxoglou, W. Whittow "A Metasurfaces Review: Definitions and Applications", Appl. Sci., 2019, 9, 2727.

[73] Z. Wu, Y. Zheng "Moiré Metamaterials and Metasurfaces", Advanced Optical Materials, 2018, 6, 1701057.

[74] P. Chieh Wu, W. Zhu, Z. Xiang Shen, P. H. Joo Chong, We. Ser, D. P. Tsai, Ai-Q. Li "Broadband Wide-Angle Multifunctional Polarization Converter via Liquid-Metal-Based Metasurface", Advanced Optical Materials, 2017, 5, 1600938.

[75] J. B. Pendry “Negative refracting makes a perfect lens”, Physical Review Letters, 2000, 85, 18, 3966-3969.

[76] V. M. Shalaev "Optical Negative-Index Metamaterials", Nature Photonics, 2007, 1, 41-48.

[77] R. Castagna, F. Vita, D. E. Lucchetta, L. Criante, L. Greci, P. Ferraris, F. Simoni "Nitroxide radicals reduce shrinkage in acrylate-based holographic gratings", Optical Materials, 2007, 30, 4, 539-544.

[78] M. Rippa, R. Castagna, M. Pannico, P. Musto, E. Bobeico, J. Zhou, and L. Petti, "High-performance Nanocavities-based Meta-crystals for Enhanced Plasmonic Sensing" Optical Data Processing and Storage, 2016; 2:22–29;

[79] S. Majee, M.F. Cerqueira, D. Tondelier, B. Geffroy, Y. Bonnassieux, P. Alpuim, and J.E. Bourée, "Flexible organic-inorganic hybrid layer encapsulation for organic opto-electronic devices", Progress in Organic Coatings, 2015, 80, 27–32.

[80] J.-H. Choi, Y.-M. Kim, Y.-W. Park, T.-H. Park, J.-W. Jeong, H.-J. Choi, E.-H. Song, J.-W. Lee, C.-H. Kim, and B.-K. Ju "Highly conformal SiO_2/Al_2O_3 nanolaminate gas-diffusion barriers for large-area flexible electronics application”, Nanotechnology, 2010, 21, 47, 475203.

[81] E.G. Jeong, Y. Jeon, S.H. Cho, and K.C. Choi "Textile-based wachable polymer solar cells for optoelectronic modules: toward self-powdered smart clothing", Energy and Environmental Science, 2019, 12, 6, 1878–1889.

[82] J. Jin, S. Chen, J. Zhang "Investigation of UV aging influences on the crystallization of ethylene-vinyl acetate copolymer via successive self-nucleation and annealing treatment", Journal of Polymer Research, 2010, 17, 827–836.

[83] J. Schlothauer, S. Jungwirth, M. Köhl, B. Röder "Degradation of the encapsulant polymer in outdoor weathered photovoltaic modules: Spatially resolved inspection of EVA ageing by fluorescence and correlation to electroluminescence", Solar Energy Materials and Solar Cells, 2012, 102, 75–85.

[84] N. Kim, W. J. Jr. Potscavage, A. Sundaramoothi, C. Henderson, B. Kippelen, S. Graham "A correlation study between barrier film performance and shelf lifetime of encapsulated organic solar cells", Solar Energy Materials and Solar Cells, 2012, 101, 140–146.

[85] Y. Fu and F.-Y. Tsai "Air-stable polymer organic thin-film transistors by solution-processed encapsulation", Organic Electronics, 2011, 12, 179–184.

[86] K. S. Ong; G. C. R. Raymond, E. Ou, Z. Zheng, D. L. M. Ying "Interfacial and mechanical studies of a composite Ag–IZO–PEN barrier film for effective encapsulation of organic TFT", Organic Electronics, 2010, 11, 463–466.

[87] Y. Jia, P. Li, X. Gui, J. Wei, K. Wang, H. Zhu, D. Wu, L. Zhang, A. Cao and Y. Xu "Encapsulated carbon nanotube-oxide-silicon solar cells with stable 10% efficiency", Applied Physics Letters, 2011, 98, 133115.

[88] X. Zang, M. Zhu, X. Li, X. Li, Z. Zhen, J. Lao, K. Wang, F. Kang, B. Wei and H. Zhu “Dynamically stretchable supercapacitors based on graphene woven fabric electrodes”, Nano Energy, 2015, 15, 83–91.

[89] J. Leem, S. Kim, S. Lee, J. Rogers, E. Kim, J. Yu "Efficiency Enhancement of Organic Solar Cells Using Hydrophobic Antireflective Inverted Moth-Eye Nanopatterned PDMS Films", Advanced Energy Materials, 2014, 4, 1301315.

[90] X. Chen, H. Lin, P. Chen, G. Guan, J. Deng, H. Peng "Smart, Stretchable Supercapacitors", Advanced Materials, 2014, 26, 4444–4449.

[91] J. Yoon, A. J. Baca, S. Park, P. Elvikis, J. B. Geddes III, L. Li, R. H. Kim, J. Xiao, S. Wang, T. Kim, M. J. Motala, B. Y. Ahn, E. B. Duoss, J. A. Lewis, R. G. Nuzzo, P. M. Ferreira, Y. Huang, A. Rockett and J. A. Rogers "Ultrathin silicon solar microcells for semitransparent, mechanically flexible and microconcentrator module designs", Nature Materials, 2008, 7, 11, 907–915.

[92] Z. Fan, H. Razavi, J. Do, A. Moriwaki, O. Ergen, Y. Chueh, P. W. Leu, J. C. Ho, T. Takahashi, L. A. Reichertz, S. Neale, K. Yu, M. Wu, J. W. Ager, A. Javey "Three-dimensional nanopillar-array photovoltaics on low-cost and flexible substrates", Nature Materials, 2009, 8, 8, 648–653.

[93] K.N. Ren, Y.Z. Zheng, W. Dai, D. Ryan, C.Y. Fung, H.K. Wu "Soft-lithography based high temperetaure molding method to fabricate whole teflon microfluidic chips", 14th International Conference on Miniaturized Systems for Chemistry and Life Sciences 3 - 7 October 2010, Groningen, The Netherlands, 554-556 (https://www.rsc.org/binaries/loc/2010/pdfs/Papers/192_0480.pdf).

[94] I. D. Johnston, D. K. McCluskey, C. K. L. Tan, M. C. Tracey "Mechanical characterization of bulk Sylgard 184 for microfluidics and microengineering", Journal of Micromechanics and Microengineering, 2014, 24, 035017.

[95] J. Lee, J. Kim, H. Kim, Y. M. Bae, K.-H. Lee, H. J. Cho "Effect of thermal treatment on the chemical resistance of polydimethylsiloxane for microfluidic devices", Journal of Micromechanics and Microengineering, 2013, 23, 035007.